Thermodynamic/Kinetic Control in the Isomerization of the $[\{t\text{BuNP}(\mu\text{-N}t\text{Bu})\}_2]^{2-}$ Ion

Andrew D. Bond,[a] Emma L. Doyle,[a] Felipe García,[a] Richard A. Kowenicki,[a] David Moncrieff,*[b] Mary McPartlin,[c] Lucía Riera,[a] Anthony D. Woods,[a] and Dominic S. Wright*[a]

Abstract: The unique structure of $[(t\text{BuN})_2\text{PK}]_\infty$ (**2**) (containing $[(t\text{BuN})_2\text{P}]^-$ monoanions) is in stark contrast to the previously reported Li^+ analogue $[\{[t\text{BuNP}(\mu\text{-N}t\text{Bu})]_2\}_2]\text{Li}_4$ (**1**) (containing the dimeric $[\{t\text{BuNP}(\mu\text{-N}t\text{Bu})\}_2]^{2-}$ ion). DFT and ^{31}P NMR spectroscopic studies reveal that the formation of the monoanion arrangements are most thermodyamically favored for Li, Na, and K, **1** being the product of kinetic control and **2** being the product of thermodynamic control.

Keywords: density functional calculations · lithium · phosphazane · potassium · sodium

Introduction

In recent years there has been considerable interest in anionic ligand arrangements containing Group 15/nitrogen frameworks.[1] The most extensively studied class of these species are the dianions $[\{\text{RNE}(\mu\text{-NR})\}_2]^{2-}$ (E = P,[2] As, Sb, Bi[1a]), which have been shown to coordinate a broad range of metal ions with retention of their dimeric E_2N_2 units.[1] For the phosphorus homologues, however, dimerization of $[(\text{RN})_2\text{P}]^-$ monoanions into $[\{\text{RNP}(\mu\text{-NR})\}_2]^{2-}$ dianions can depend on the steric demands of the organic substituents (R) (Scheme 1). Thus, the complex $[\{[t\text{BuNP}(\mu\text{-N}t\text{Bu})]_2\}_2]\text{Li}_4$ (**1**) (Scheme 2a) contains $[\{t\text{BuNP}(\mu\text{-N}t\text{Bu})\}_2]^{2-}$ ions,[2b] whereas $[\{[\text{R(Mes)N}]_2\text{PLi}\}_2]$ (Mes = 2,4,6-$Me_3C_6H_2$; R = 1-adamantyl, *t*Bu) contain $[\{\text{R(Mes)N}\}_2\text{P}]^-$ ions (Scheme 2b).[3]

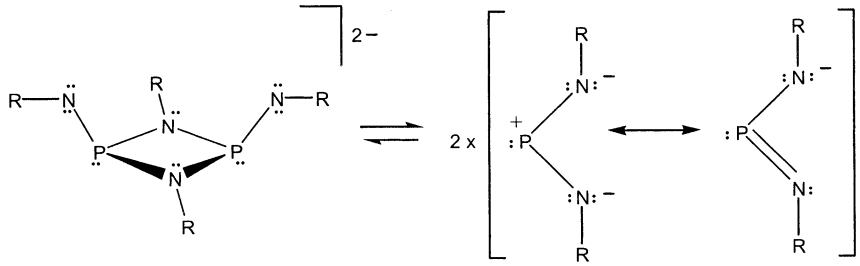

Scheme 1. Notional equilibrium between the $[\{\text{RNP}(\mu\text{-NR})\}_2]^{2-}$ ion and $[(\text{RN})_2\text{P}]^-$ ions.

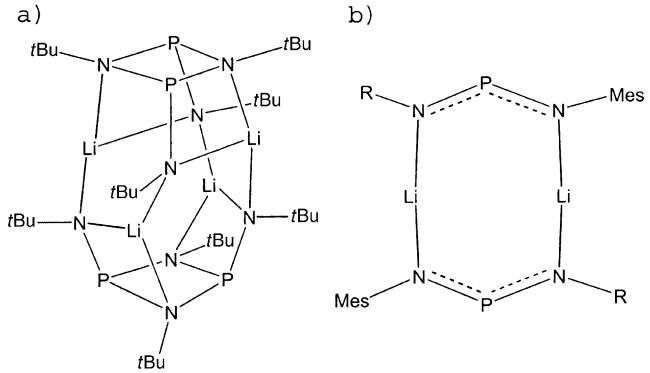

Scheme 2. a) Structure of the 'double-cubane' aggregate $[\{[t\text{BuNP}(\mu\text{-N}t\text{Bu})]_2\}_2]\text{Li}_4$ (**1**); b) Structure of $[\{[\text{R(Mes)N}]_2\text{PLi}\}_2]$ (Mes = 2,4,6-$Me_3C_6H_2$; R = 1-adamantyl, *t*Bu).

[a] Dr. A. D. Bond, Dr. E. L. Doyle, F. García, R. A. Kowenicki, Dr. L. Riera, Dr. A. D. Woods, Dr. D. S. Wright
Chemistry Department, University of Cambridge
Lensfield Road, Cambridge CB2 1EW (UK)
Fax: (+44) 1223-336362
E-mail: dsw1000@cus.cam.ac.uk.

[b] Dr. D. Moncrieff
School of Computational Science & Information Technology
Florida State University, Tallahassee, FL 32306–4120 (USA)

[c] Prof. M. McPartlin
Department of Health and Human Sciences
London Metropolitan University
Holloway Road, London N7 8DB (UK)

 DOI: 10.1002/chem.200305762

In rare cases sterically uncongested dianions can undergo ring opening into monoanions. The coordination requirements of Ga^{III} have been invoked to explain the presence of a $[(t\text{BuN})_2\text{P}]^-$ ion in $[\{\text{PhNP}(\mu\text{-NPh})\}_2\text{Ga}\{\text{P}(\text{N}t\text{Bu})_2\}]$[4] (Scheme 3a), whereas the presence of intramolecular Lewis base functionality results in trapping of this anion in $[\{t\text{BuNP}(\mu\text{-N}t\text{Bu})_2\text{PN(2-py)}\}\text{Li}_2\{\text{LiP}(\text{N}t\text{Bu})_2\}]$ (2-py = 2-pyridyl)(Scheme 3b).[5]

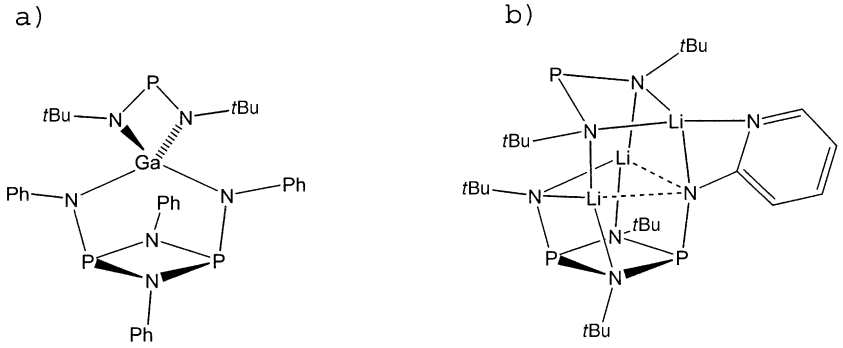

Scheme 3. Structures of a) $[\{\text{PhNP}(\mu\text{-NPh})\}_2\text{Ga}\{\text{P}(\text{N}t\text{Bu})_2\}]$ and b) $[\{t\text{BuNP}(\mu\text{-N}t\text{Bu})_2\text{PN(2-py)}\}\text{Li}_2\{\text{LiP}(\text{N}t\text{Bu})_2\}]$ (2-py = 2-pyridyl), containing the $[(t\text{BuN})_2\text{P}]^-$ ion.

We report here the surprising discovery that the reactions of $[\{t\text{BuN(H)P}(\mu\text{-N}t\text{Bu})\}_2]$ with BnM (M = Na, K) in toluene result *exclusively* in the formation of the $[(t\text{BuN})_2\text{P}]^-$ ion. In situ NMR spectroscopic studies and DFT calculations indicate that the selection of the $[(t\text{BuN})_2\text{P}]^-$ ion in the heavier alkali-metal complexes is thermodynamically controlled, whereas the formation of the $[\{t\text{BuNP}(\mu\text{-N}t\text{Bu})\}_2]^{2-}$ ion in the previously reported Li derivative is kinetically controlled.

Results and Discussion

The reaction of the macrocyclic aminophosphazane $\{[\text{P}(\mu\text{-N}t\text{Bu})]_2\text{NH}\}_4]$[6] with excess BnK (8 equiv) (Bn = CH_2Ph) in toluene at reflux was undertaken in an attempt to obtain the tetraanion $[\{[\text{P}(\mu\text{-N}t\text{Bu})]_2\text{N}\}_4]^{4-}$, by deprotonation of the four N-H protons within the ring (Scheme 4). However, $[(t\text{BuN})_2\text{PK}]_\infty$ (**2**) was isolated unexpectedly as the major product, resulting from the fragmentation of the P–N-bonded arrangement of the precursor. Although the mechanism of this reaction is unknown, we attribute this outcome to the low acidity of the N-H protons, which results from shielding of the macrocyclic core by the *t*Bu periphery. For example, $[\{[\text{P}(\mu\text{-N}t\text{Bu})]_2\text{NH}\}_4]$ is unreactive towards a range of organoalkali metal reagents (such as MeLi or *t*BuLi) at room temperature or under reflux in toluene.

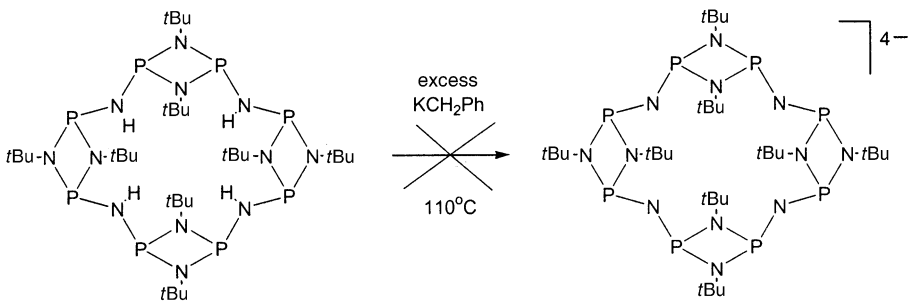

Scheme 4. Attempted reaction of the tetramer $[\{\text{P}(\mu\text{-N}t\text{Bu})\}_2(\mu\text{-NH})]_4$ with $PhCH_2K$.

Intrigued by the formation of a $[(t\text{BuN})_2\text{P}]^-$ ion in **2**, we undertook the reaction of $[\{t\text{BuN(H)P}(\mu\text{-N}t\text{Bu})\}_2]$[2a] with excess BnK (1:8 equiv, respectively). No reaction occurs at room temperature in toluene. However, under prolonged (12 h) reflux **2** is generated almost exclusively (Scheme 5), as shown by in situ ^{31}P NMR studies of the reaction mixture. The room-temperature ^{31}P NMR spectra of reaction solutions consist of a singlet at $\delta = 356.7$ ppm for the $[(t\text{BuN})_2\text{P}]^-$ ion, with little or none of $[\{t\text{BuN(H)P}(\mu\text{-N}t\text{Bu})\}_2]$ remaining (ca. $\delta = 89.6$ ppm) and with none of the $[\{t\text{BuNP}(\mu\text{-N}t\text{Bu})\}_2]^{2-}$ ion being present (ca. $\delta = 125$ ppm[2b]) (in toluene/[D_6]acetone capillary). Chemical shifts of about $\delta = 340$–395 ppm have been observed previously for $[(\text{RN})_2\text{P}]^-$ ions.[2–5] The highly deshielded nature of the P centers in these species has been used to suggest a charge-separated, N^--P^+-N^- structure for the monoanions.[7a] However, more recent studies have indicated that the high values of the chemical shifts may result from more complicated effects, such as efficient mixing of the P lone pair and π* orbitals in the N=P=N framework.[7b,c] The formation of a $[(t\text{BuN})_2\text{P}]^-$ ion in **2** contrasts dramatically with the formation of the $[\{t\text{BuNP}(\mu\text{-N}t\text{Bu})\}_2]^{2-}$ ion in the room-temperature lithiation of $[\{t\text{BuN(H)P}(\mu\text{-N}t\text{Bu})\}_2]$ with *n*BuLi (complex **1**, Scheme 2a).[2b] Complex **2** is highly moisture-sensitive and despite repeated attempts, using flame-dried glassware and rigorous inert-atmosphere procedures, **2** could only be isolated as a solid contaminated by small amounts of the starting material $[\{t\text{BuN(H)P}(\mu\text{-N}t\text{Bu})\}_2]$, which is always generated during filtration and handling. Prolonged storage of toluene solutions during crystallisation also resulted in the generation of $[\{t\text{BuN(H)P}(\mu\text{-N}t\text{Bu})\}_2]$ together with **2**, possibly as a consequence of deprotonation of solvent. For this reason satisfactory elemental analysis could not be obtained.

$$[t\text{BuN(H)P}(\mu\text{-N}t\text{Bu})]_2 \xrightarrow[\text{toluene/ } 110^\circ\text{C}]{\text{excess BnK}} [(t\text{BuN})_2\text{PK}]_\infty$$

Scheme 5. Formation of **2**.

An in situ ^{31}P NMR spectroscopic study of the reaction of $[\{t\text{BuN(H)P}(\mu\text{-N}t\text{Bu})\}_2]$ with excess $PhCH_2Na$ in toluene using the same procedure as for **2** also showed the exclusive formation of the $[(t\text{BuN})_2\text{P}]^-$ ion ($\delta = 367.0$) (+25 °C in toluene/[D$_6$]acetone capillary). Intrigued by a previous brief report that prolonged reflux of $[\{t\text{BuN(H)P}(\mu\text{-N}t\text{Bu})\}_2]$ with *n*BuLi (1:2 molar equivalents) gives the cage $[\text{Li}_2\{t\text{BuNP}(\mu\text{-N}t\text{Bu})\}_2]_2[\{(t\text{BuN})_2\text{P}\}\text{Li}]$, consisting of a $[\{t\text{BuNP}(\mu\text{-N}t\text{Bu})\}_2]^{2-}$ ion and a $[\{t\text{BuN})_2\text{P}\}]^-$ ion,[1b,8] we decided to re-investigate the Li system. The in situ ^{31}P NMR spectrum of the reaction solution formed by the addition of $[\{t\text{BuN(H)P}(\mu\text{-N}t\text{Bu})\}_2]$ to *n*BuLi (1:2 molar equivalents)[2b] at 0 °C in toluene ([D$_6$]acetone capillary) shows the almost quantitative formation of $[\{[t\text{BuNP}(\mu\text{-N}t\text{Bu})]_2\}_2]\text{Li}_4$ (**1**). However, after 16 h reflux resonances characteristic of the $[(t\text{BuN})_2\text{P}]^-$ ion are observed ($\delta = 376.3$–392.3 ppm), together with those of other species including the cyclic phosphazane $[\{[\text{P}(\mu\text{-N}t\text{Bu})]_2(\mu\text{-N}t\text{Bu})\}_2]$[2b] as a major product ($\delta =$ 119.4 ppm). The presence of three resonances in the $[(t\text{BuN})_2\text{P}]^-$ region [at $\delta = 392.3$(s), 381.2 (s) (minor), 376.3 ppm (s)], suggests that more than one Li complex of this ligand is generated. Further reflux (up to 40 h) results in more of **1** being converted into the monoanion and $[\{[\text{P}(\mu\text{-N}t\text{Bu})]_2(\mu\text{-N}t\text{Bu})\}_2]$ (the overall conversion of **1** into other products being about 50 % as determined by integration of the spectrum). The results on the Na and K systems indicate that the $[(t\text{BuN})_2\text{P}]^-$ ion is thermodynamically more stable than the dianion counterpart. In the case of Li, the rate of conversion of the dianion into the monoanion is considerably slower and the reaction is far less selective. Nonetheless, the NMR spectroscopic study of the reaction of *n*BuLi with $[\{t\text{BuN(H)P}(\mu\text{-N}t\text{Bu})\}_2]$ suggests that the $[(t\text{BuN})_2\text{P}]^-$ ion is thermodyamically preferred to the dianion.

To provide further support for the conclusions drawn primarily from NMR spectroscopic studies, the low-temperature X-ray structure on **2** was obtained. Despite repeated attempts, crystals of the Na analogue could not be grown. Details of the data collection and refinement of **2** are listed in Table 1, with Table 2 giving selected bond lengths and angles.

Table 1. Crystal data and refinement of $[(t\text{BuN})_2\text{PK}]_\infty$ (**2**).

formula	$C_8H_{18}KN_2P$
MW	212.31
crystal system	cubic
space group	$Im\bar{3}$
Z	12
a [Å]	15.9435(18)
V [Å^3]	4052.8(8)
$\mu(\text{Mo}_{K\alpha})$ [mm^{-1}]	0.474
ρ_{calcd} [Mg m^{-3}]	1.044
T [K]	180(2)
total reflections	7521
unique reflections (R_{int})	375 (0.068)
$R1$, $WR2$ [$I > 2\sigma(I)$]	0.0437, 0.1275
$R1$, $WR2$ (all data)	0.0509, 0.1339

Table 2. Selected bond lengths [Å] and angles [°] for $[(t\text{BuN})_2\text{PK}]_\infty$ (**2**).

K(1)–N(1,1B)	2.909(4)	P(1)–N(1,1B)	1.587(5)
K(1F,1)–P(1,1C)	3.342(3)		
N(1)-K(1)-N(1B)	51.6(2)	K(1)-N(1)-K(1A)	66.8(1)
N(1)-K(1)-N(1D)	90.9(2)	N(1)-P(1)-N(1B)	105.9(4)
N(1)-K(1)-N(1A)	113.2(1)		

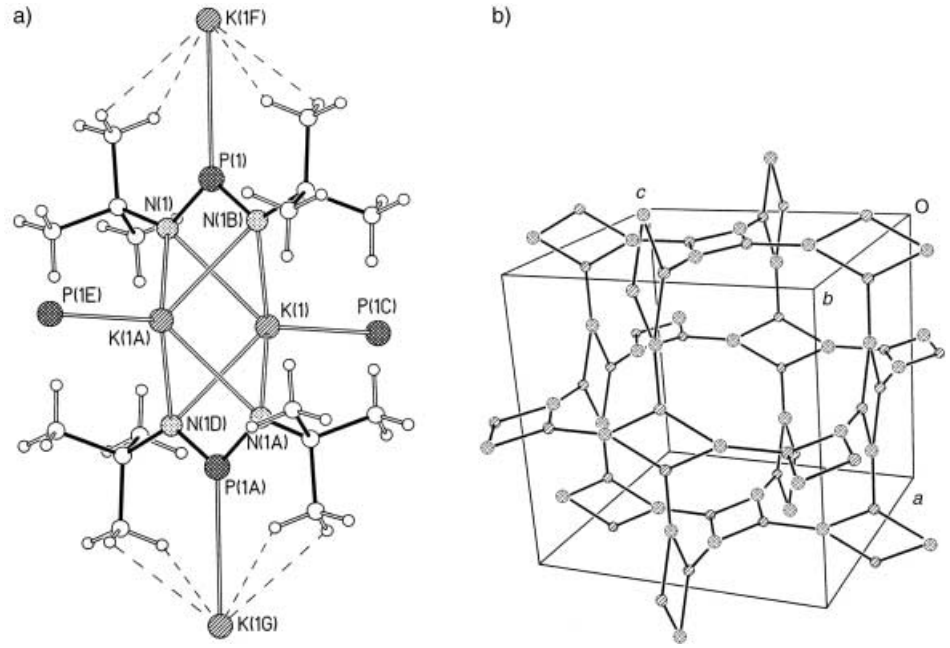

Figure 1. a) $[(t\text{BuN})_2\text{PK}]_2$ dimer units in **2**. Symmetry used to generate atoms: A: $1-x$, $1-y$, $-z$; B: x, y, $-z$; C: $^1/_2-z$, $^1/_2-x$, $^1/_2-y$; D: $1-x$, $1-y$, z; E: $^1/_2+z$, $^1/_2+x$, $-^1/_2+y$; F: $^1/_2-y$, $^1/_2-z$, $^1/_2-x$; G: $^1/_2+y$, $^1/_2+z$, $-^1/_2+x$. b) Architecture of the lattice, showing one unit cell (phosphorus and potassium atoms only shown; N, C and H atoms are omitted for clarity).

The structure of **2** shows that the complex is constructed from $[\{(t\text{BuN})_2\text{PK}\}_2]$ dimer units (Figure 1a) in which the two symmetry-related K^+ ions are μ_2-bridged by both of the N centers of each of the $[(t\text{BuN})_2\text{P}]^-$ ions (K(1)–N(1) 2.909(4) Å). These dimers then associate into an elaborate three-dimensional network by bonding of each of the K^+ ions to the P center of a neighboring $[(t\text{BuN})_2\text{P}]^-$ ion [K(1)–P(1C), K(1F)–P(1) 3.342(3) Å (Figure 1a and 1b)]. The association of the dimer units is reinforced by relatively short, agostic C(-H)···K interactions (3.55 Å) with the Me groups of these anions (ca. 3.5–4.0 Å in a range of organopotassium compounds[9]). Despite the previous suggestion of high positive charge carried by the P atom in $[(\text{RN})_2\text{P}]^-$

ions,[2–5,7a] the K–P contacts linking the dimer units in **2** (3.342(3) Å) are typical of those observed in structurally characterized K phosphides (range ca. 3.23–3.66 Å[10]). The involvement of the P centers in metal bonding is a particularly novel feature of **2** that has not previously been found in *any* metal complex containing $[(RN)_2P]^-$ ions.

DFT (B3LYP) calculations[11] were performed on the monoanion species $[\{(t\text{BuN})_2\text{PM}\}_2]$ (M = Li, (**1a**); K (**2a**)), the cubanes $[\{t\text{BuNP}(\mu\text{-N}t\text{Bu})\}_2\text{M}_2]$ (M = Li, (**1b**); K (**2b**)), and the double-cubanes $[\{[t\text{BuNP}(\mu\text{-N}t\text{Bu})\}_2\text{M}_2\}_2]$ (M = Li, (**1**); K (**2c**)) (all at 298.15 K). Owing to the complexity of these calculations and to the computer time required, calculations on the Na systems were not undertaken. Geometry optimizations and frequency analyses were performed using the Gaussian 98 software program.[11a] A cc-pvdz[11b] basis set was employed for all atoms in the dimer and cubane molecules. The lithium and potassium basis sets were obtained from the Extensible Computational Chemistry Environment Basis Set Database.[11c] The DFT optimizations and frequency calculations were performed using a B3LYP[12d] functional employing the INT = ULTRAFINE parameter to define the numerical grid.

Figure 2 shows the geometry-optimized structures of the Li species **1**, **1a**, and **1b** and the K species **2a**–**2c**, together with selected bond lengths and angles. Optimization of **1** was performed by using the coordinates obtained from the X-ray data on the complex as a starting point. The geometry-optimized structure is very similar to that found experimentally,[2b] consisting of the association of two cubane units and with a tetrahedral arrangement of the four Li^+ ions at the center of the cage. Although the calculated P–N bond lengths in the $[\{t\text{BuNP}(\mu\text{-N}t\text{Bu})\}_2]^{2-}$ ions of **1** (terminal P–N 1.836–1.844 Å, bridging P–μ-N 1.698–1.698 Å) are longer than those found in the X-ray structure (terminal P–N 1.743(9)–1.797(9) Å, P–μ-N 1.644(9)-1.655(9) Å), the calculated N–Li bond lengths (range 2.062–2.160 Å), the P-N-P (96.5°) and N-P-N [82.7°] angles within the P_2N_2 ring units, and the exocyclic μ-N-P-N(*t*Bu) angles (101.0–107.4°) are all very similar to those found in the experimental structure (cf. N–Li range 2.03(3)–2.19(3) Å, P-N-P range 96.0(4)–98.2(5)°, N-P-N 81.7(4)–83.3(6)°, exocyclic μ-N-P-N(*t*Bu) range 103.0(4)–105.0(5)°).[2b] Optimization of the K analogue **2c** was undertaken using the coordinates of **1** as the starting point, by replacing the Li^+ ions with K^+ ions. There is no

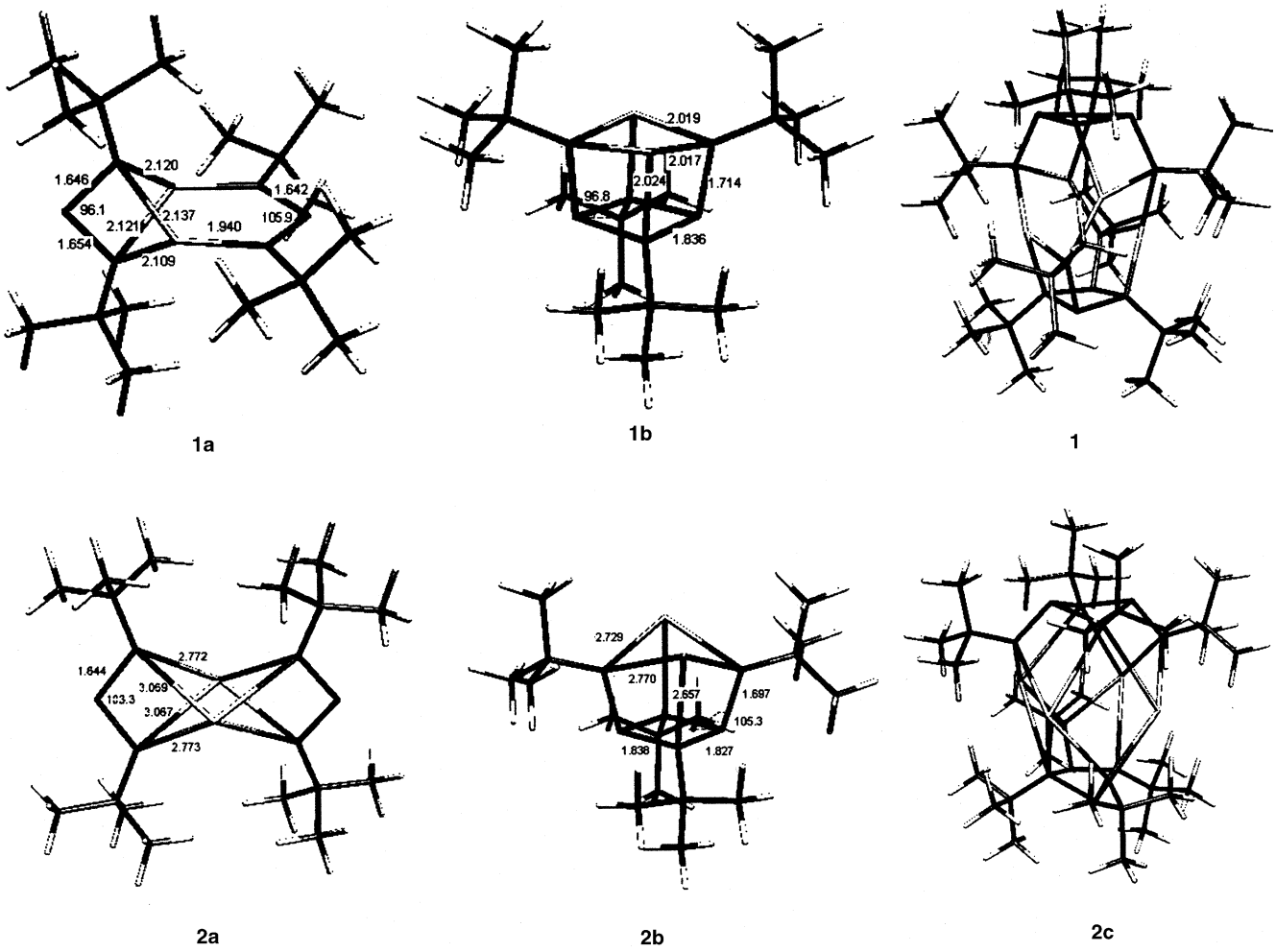

Figure 2. DFT (B3LYP) geometry-optimized structures of $[\{(t\text{BuN})_2\text{PM}\}_2]$ (M = Li (**1a**); M = K (**2a**)), $[\{t\text{BuNP}(\mu\text{-N}t\text{Bu})\}_2\text{M}_2]$ (M = Li (**1b**); M = K (**2b**)), and $[\{[t\text{BuNP}(\mu\text{-N}t\text{Bu})]_2\text{M}_2\}_2]$ (M = Li (**1**); M = K (**2c**)). Bond lengths [Å] and angles [°] for **1**: μ-N–P 1.838–1.844, $N_{terminal}$–P 1.697–1.698, μ-N–Li 2.158–2.160, $N_{terminal}$–Li 2.062–2.071; N-μ-P-N 82.7, P-μ-N-P 96.5, N-P-N*t*Bu 101.0–107.4. For **2c**: μ-N–K 3.293–3.284, N–K 2.695–2.606, K···K 3.613–3.614, N-μ-P-N 79.8, P-μ-N-P 93.7.

experimental data available on **2c**; however, the geometry-optimized structure of this species is strikingly similar in its architecture to those of $[\{\text{CyNE}(\mu\text{-NCy})\}_2]_2\text{Na}_4]$ (Cy = cyclohexyl; E = As,[12a] Sb[12b]), containing a square-planar Na_4 arrangement at the center of the cage. This arrangement contrasts with the tetrahedral pattern found in the Li complexes $[\{\text{CyNE}(\mu\text{-NCy})\}_2]_2\text{Li}_4]$[12c,d] which have similar solid-state structures to **1**, and has been attributed to the effect of the increase in the ionic radius of the coordinated metal ion. Thus, the optimized structure of **2c** is entirely consistent with previous experimental observations concerning the structural changes occurring in this type of double-cubane cage for the heavier alkali metals. Geometry optimization of the K mononanion species **2a** was performed using the experimental coordinates of the units found in the X-ray structure of **2** as the starting geometry. The most stable calculated structure of this isolated species is similar to the units found in the solid-state structure of **2**, however, in the calculated model the N-P-N planes of the two $[(t\text{BuN})_2\text{P}]^-$ anions are staggered by 24.2° with respect to each other (rather than being eclipsed, as in the experimental crystal structure of **2**). This arrangement results in an unsymmetrical pattern of N–K bond lengths in **2c** (N–K 2.772–3.069 Å) compared to uniform N–K bond lengths found in the units of **2** in the solid state (N–K 2.909(4) Å). The adoption of a staggered arrangement in **2a** appears to be the result of steric repulsion between the *t*Bu groups of the two $[(t\text{BuN})_2\text{P}]^-$ ligands. The calculations on the analogous Li species **1a** (using the experimental coordinates for **2** as the starting geometry and replacing K^+ with Li^+) give a very different arrangement to that found in the K monoanion model **2a**. The presence of shorter Li–N bonds in **1a** results in increased steric repulsion between the two $[(t\text{BuN})_2\text{P}]^-$ ligands than occurs in **2a**, and in the adoption of a completely staggered arrangement (in which the planes of the N-P-N units are approximately perpendicular). The adoption of two different bonding modes for the $[(t\text{BuN})_2\text{P}]^-$ ions (μ-N/μ-N and terminal-N/terminal-N) is of interest in regard to the structures of the dimers $[\{[\text{R(Mes)N}]_2\text{PLi}\}_2]$ (Mes = 2,4,6-$Me_3C_6H_2$; R = 1-adamantyl, *t*Bu)[3] mentioned previously (Figure 2b). In the latter, only a terminal-N/terminal–N bonding mode is observed for both monoanion ligands owing to the presence of even greater steric crowding in these complexes.

Figure 3 shows the thermodynamic data obtained from the DFT calculations, and the values of ΔE, ΔH, and ΔG for the interconversions between the various models for Li and K. The relative stabilities found for the Li and K models are both in the order monoanion > double-cubane > cubane. Although the association of cubanes **1b** into the double-cubane **1** is accompanied by a favorable enthalpy change ($\Delta H = -6.5$ kcal mol^{-1}), this is outweighed by an unfavorable entropy change, making this association thermodynamically disfavored ($\Delta G = +12.6$ kcal mol^{-1}). In contrast, the alternative rearrangement **1b**→**1a** is highly thermodynamically favorable on both entropic and enthalpic grounds ($\Delta G = -25.2$ kcal mol^{-1}). There is a marginally greater preference for the monoanion model **2a** for the K systems than is found for the Li analogue (**1a**) (i.e., $\Delta G = -41.5$ kcal mol^{-1} for **2c**→2×**2a**, cf -37.8 kcal mol^{-1} for **1**→2×**1a**). It can be noted, however, that the self-assembly of the relatively unhindered K species **2a** into the three-dimensional network of **2** would result in an increase in coordination number of K^+ to five and would undoubtedly lead to an even greater thermodynamic preference for this arrangement. In contrast, this option is unlikely for the Li counterpart **1a** since intermolecular P–Li association (in a manner akin to that occurring for **2** in the solid state) will be disfavored by steric shielding of the Li^+ ions.

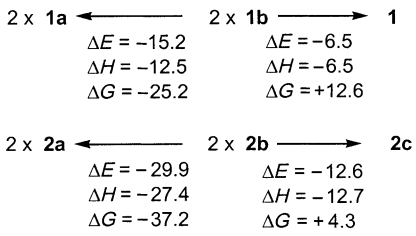

Figure 3. Interconversion of the Li models (**1a**, **1b**, and **1**) and the K models (**2a**, **2b**, and **2c**) (units in kcal mol^{-1}).

Conclusion

The combined results of in situ NMR spectroscopic studies and DFT calculations show that the monoanion arrangement of **2** is thermodynamically controlled. However, the formation of the dianion arrangement in the previously reported complex **1** is kinetically controlled. This could be as a result a lower overall activation energy for association of 2×**1b**→**1** compared to the cycloreversion **1b**→**1a**. This study highlights the potentially broad importance of thermodynamic *and* kinetic control on the structures of anionic Group 15/nitrogen frameworks for the first time.

Experimental Section

All manipulations were carried out under dry argon. Glassware was flame dried. Toluene was freshly distilled over Na/benzophenone. $[\{t\text{BuN(H)P}(\mu\text{-N}t\text{Bu})\}_2]$ was prepared by using the literature method, from the reaction of PCl_3 and $t\text{BuNH}_2$.[2a] In situ ^{31}P NMR studies on reaction mixtures were undertaken using a Bruker AM400 NMR spectrometer. Samples were withdrawn from reactions by syringe and placed in thin-walled, 528pp NMR tubes together with a $[D_6]$acetone capillary in order to obtain a lock. Samples were referenced to 85% H_3PO_4 in D_2O. A Perkin-Elmer Paragon 1000 spectrophotomer was used in IR studies.

Synthesis of 2: In a typical reaction $[\{t\text{BuN(H)P}(\mu\text{-N}t\text{Bu})\}_2]$ (2.0 g, 5.74 mmol) in toluene (100 mL) was added to a suspension of $PhCH_2K$ (6.0 g, 46.1 mmol) in toluene (100 mL). The mixture was stirred at room temperature (2 h) then brought to reflux (12 h). The mixture was filtered (Celite, P3) to give an orange solution. The solvent was removed under vacuum to give **2** as a tan-colored solid. Yield 0.72 g (59% based on $[\{t\text{BuN(H)P}(\mu\text{-N}t\text{Bu})\}_2]$ supplied). The contamination of this material with small amounts of $[\{t\text{BuN(H)P}(\mu\text{-N}t\text{Bu})\}_2]$ made it impossible to obtain satisfactory elemental analysis. NMR spectroscopic investigations were undertaken using solvents that were dried using a Na mirror and degassed prior to use. IR (Nujol, NaCl): $\tilde{\nu}$ [cm^{-1}] = 1200 s, 1121 s, 1014 s, 922 w, 839 s, 747 m, 726 m, 704 w (air-exposure gave a sharp band at 3676 cm^{-1} for K–OH str. and a collection of weak N–H str. bands (3726–3341 cm^{-1}) for $[\{t\text{BuN(H)P}(\mu\text{-N}t\text{Bu})\}_2]$, with the rest of the spectrum being almost identical to that for **2** apart from the band at 1200 cm^{-1}

shifting to 1216 cm^{-1} and that at 1121 cm^{-1} shifting to 1088 cm^{-1}). ^1H NMR (400 MHz, [D_6]benzene, +25 °C): $\delta = 1.54$ (s) (cf. $\delta = 1.11$ ppm (d., $^3J_{PH} = 0.2$ Hz, major) in toluene with [D_6]acetone capillary) (*t*Bu, **2**); $^{31}P\{^1H\}$ NMR (161.975 MHz, [D_6]benzene, +25 °C), $\delta = 356.7$ (s) (major, **2**) (cf. $\delta = 354.0$ ppm in toluene with [D_6]acetone capillary), 90.8 ppm (s) (minor [{*t*BuN(H)P(μ-N*t*Bu)}$_2$]) (cf. $\delta = 89.6$ ppm in toluene with [D_6]acetone capillary). Crystals of **2** are obtained in low yield by prolonged storage of toluene solutions at −20 °C (several weeks). This commonly also produces crystals of [{*t*BuN(H)P(μ-N*t*Bu)}$_2$] as a result of hydrolysis or deprotonation of the solvent.

In situ NMR studies of the Li and Na systems: The reaction of [{*t*BuN(H)P(μ-N*t*Bu)}$_2$] with *n*BuLi was performed in the manner described in reference[2b]. NMR samples were withdrawn by using a syringe, and a [D_6]acetone capillary was used to obtain a lock. All $^{31}P\{^1H\}$ spectra were recorded at 0 °C (161.975 MHz) to resolve the resonances for *intact* **1** from those for the cubane **1b** (as noted in reference [2b]). Initial reaction mixture: $\delta = 131.2$ (s) [{*t*BuNP(μ-N*t*Bu)}$_2$Li$_2$] (**1b**) (lit. [D_8]toluene, ca. $\delta = 128$[2b]), 127.5 (s) *intact* [{[*t*BuNP(μ-N*t*Bu)]$_2$}$_2$]Li$_4$ (**1**) (lit. [D_8]toluene, ca. $\delta = 125$[2b]), other minor resonances at $\delta = 129.2$–128.8 and 162.3 ppm (s). After 40 h reflux: $\delta = 392.3$ (s), 381.2 (s) (minor), 376.3 (s), 181.0 (d) (12.4 Hz), 99.4 (d) (12.4 Hz), 160.5 (s) 129.4 (s), 129.1 (s), 127.3 (s), 119.4 (s) [{[P(μ-N*t*Bu)]$_2$(μ-N*t*Bu)}$_2$] (lit. [D_8]toluene, 117.2[2b]), other minor resonances $\delta = 76.2$–6.0 ppm.

The reaction of BnNa with [{*t*BuN(H)P(μ-N*t*Bu)}$_2$] (8:1 molar equivalents) was carried out in exactly the same way as the method used for **2** (using the same scale, duration and temperature). $^{31}P\{^1H\}$ NMR (+25 °C, toluene/[D_6]acetone capillary), $\delta = 367.0$ ppm (s) (no other resonances).

X-ray crystallography on 2: Data were collected on a Nonius KappaCCD diffractometer. The structure was solved by direct methods and refined by full-matrix least squares on F^2.[13] CCDC-218517 contains the supplementary crystallographic data for this paper. These data can be obtained free of charge via www.ccdc.can.ac.uk/conts/retrieving.html (or from the Cambridge Crystallographic Center, 12 Union Road, Cambridge CB21EZ, UK; Fax: (+44) 1223-336033; or deposit@ccdc.cam.ac.uk).

Acknowledgement

We thank the EPSRC (A.D.B., E.L.D. F.G., M.McP., D.S.W), the EU (fellowship for L.R.), St. Catharine's College, Cambridge (fellowship for A.D.W.), The States of Guernsey and The Domestic and Millennium Fund (R.A.K.), and The Cambridge European Trust (F.G.) for financial support. We also thank Dr. J. E. Davies (Cambridge) for collecting X-ray data for compound **2**.

[1] a) M. A. Beswick, D. S. Wright, *Coord. Chem. Rev.* **1998**, *176*, 373; b) L. Stahl, *Coord. Chem. Rev.* **2000**, *210*, 203; c) J. K. Brask, T. Chivers, *Angew. Chem.*, **2001**, *114*, 3618; *Angew. Chem. Int. Ed.* **2001**, *40*, 3960, references therein.

[2] a) I. Schranz, L. Stahl , R. J. Staples, *Inorg. Chem.* **1998**, *37*, 1493; b) J. K. Brask, T. Chivers, M. L. Krahn, M. Parvez, *Inorg. Chem.* **1999**, *38*, 290.

[3] R. Detsch, E. Niecke, M. Nieger, W. W. Schoeller, *Chem. Ber.* **1992**, *125*, 1119.

[4] I. Schranz, D. F. Moser, L. Stahl, R. J. Staples, *Inorg. Chem.* **1999**, *38*, 5814.

[5] A. D. Bond, E. L. Doyle, S. J. Kidd, A. D. Woods, D. S. Wright, *Chem. Commun.* **2001**, 777.

[6] A. Bashall, E. L. Doyle, C. Tubb, S. J. Kidd, M. McPartlin, A. D. Woods, D. S. Wright, *Chem. Commun.* **2001**, 2542.

[7] a) P. B. Hitchcock, H. A. Jasim, M. F. Lappert, H. D. Williams, *J. Chem. Soc. Chem. Commun.* **1986**, 2452; b) D. Gudat, W. Hoffbauer, E. Niecke, W. W. Schoeller, U. Fleischer, W. Kutzelnigg, *J. Am. Chem. Soc.* **1994**, *116*, 7325; c) N. Burford, T. S. Cameron, J. A. C. Clyburne, K. Eichele, K. N. Robertson, S. Sereda, R. E. Wasylishen, W. A. Whitla, *Inorg. Chem.* **1996**, *35*, 5460.

[8] No further structural or experimental detail on this complex has been reported, cited in ref. [1b] as unpublished results.

[9] C. Schade, P. von R. Schleyer *Adv. Organomet. Chem.*, **1987**, *27*, 169, and references therein.

[10] Search of the Cambridge Crystallographic Data Base (August 2003).

[11] a) Gaussian 98 (Revision A.7), M. J. Frisch, G. W. Trucks, H. B. Schlegel, G. E. Scuseria, M. A. Robb, J. R. Cheeseman, V. G. Zakrzewski, J. A. Montgomery, R. E. Stratmann, J. C. Burant, S. Dapprich, J. M. Millam, A. D. Daniels, K. N. Kudin, M. C. Strain, O. Farkas, J. Tomasi, V. Barone, M. Cossi, R. Cammi, B. Mennucci, C. Pomelli, C. Adamo, S. Clifford, J. Ochterski, G. A. Petersson, P. Y. Ayala, Q. Cui, K. Morokuma, D. K. Malick, A. D. Rabuck, K. Raghavachari, J. B. Foresman, J. Cioslowski, J. V. Ortiz, B. B. Stefanov, G. Liu, A. Liashenko, P. Piskorz, I. Komaromi, R. Gomperts, R. L. Martin, D. J. Fox, T. Keith, M. A. Al-Laham, C. Y. Peng, A. Nanayakkara, C. Gonzalez, M. Challacombe, P. M. W. Gill, B. G. Johnson, W. Chen, M. W. Wong, J. L. Andres, M. Head-Gordon, E. S. Replogle, J. A. Pople, Gaussian, Inc., Pittsburgh, PA, **1998**; b) T. H. Dunning, Jr., *J. Chem. Phys.* **1989**, *90*, 1007; D. E. Woon, T. H. Dunning, Jr., *J. Chem. Phys.* **1993**, *98*, 1358. Basis sets were obtained from the Extensible Computational Chemistry Environment Basis Set Database, Version 6/19/03, as developed and distributed by the Molecular Science Computing Facility, Environmental and Molecular Sciences Laboratory which is part of the Pacific Northwest Laboratory, P. O. Box 999, Richland, Washington 99352, USA, and funded by the U. S. Department of Energy. The Pacific Northwest Laboratory is a multi-program laboratory operated by Battelle Memorial Institue for the U. S. Department of Energy under contract DE-AC06–76RLO 1830. Contact David Feller or Karen Schuchardt for further information; d) A. D. Becke, *J. Chem. Phys.* **1993**, *104*, 1040.

[12] a) A. Bashall, M. A. Beswick, C. N. Harmer, A. D. Hopkins, M. McPartlin, M. A. Paver, P. R. Raithby, A. Steiner, D. S. Wright, *J. Chem. Soc. Dalton Trans.* **1998**, 1389; b) A. Bashall, M. A. Beswick, E. A. Harron, A. D. Hopkins, S. J. Kidd, M. McPartlin, P. R. Raithby, A. Steiner, D. S. Wright, *Chem. Commun.* **1999**, 1145; c) A. J. Edwards, M. A. Paver, M.-A. Rennie, C. A. Russell, P. R. Raithby, D. S. Wright, *J. Chem. Soc. Chem. Commun.* **1994**, 1481; d) M. A. Beswick, E. A. Harron, A. D. Hopkins, P. R. Raithby, D. S. Wright, *J. Chem. Soc. Dalton Trans.* **1999**, 107.

[13] G. M. Sheldrick, SHELX-97, Göttingen, Germany, 1997.

Received: November 28, 2003
Revised: February 2, 2004 [F5762]